AIVTS 2025

The First International Conference on AI-enabled Unmanned Autonomous Vehicles and Internet of Things for Critical Services

ISBN: 978-1-68558-317-0

October 26th - 30th, 2025

Barcelona, Spain

AIVTS 2025 Editors

Jyrki Penttinen, Alphacore Inc., USA

AIVTS 2025

Forward

The First International Conference on AI-enabled Unmanned Autonomous Vehicles and Internet of Things for Critical Services (AIVTS 2025), held on October 26-30, 2025 in Barcelona, Spain, inaugurated a series of events focusing on advanced topics on integrating IoT, UAV and AI/ML and target solutions for dynamic and critical systems.

The rapid advances and widespread adoption of the Internet of Things (IoT) have promoted a revolution in communication and processing technology and offered a very large range of applications and services. Multi emerging directions in systems design and implementation are developed. IoT systems have advanced greatly in the past few years, becoming intelligent, especially with the support of Artificial Intelligence (AI) and Machine Learning (ML).

In parallel, Unmanned Autonomous Vehicles (UAVs) technology (aerial drones, terrestrial, underearth, and underwater), enabled new applications in various areas such as energy, agriculture, transportation, avionic, health, military, surveillance and monitoring, delivery, critical missions and others. Multi-UAVs solutions allowed systems to collaborate and complete missions more efficiently and economically. One particular UAV domain concerns both autonomy and automation, because of challenges of secure and reliable connectivity and privacy preservation. Integration of AI/ML in UAVs can lead to high growth in the field, by improving safety and efficiency. ML algorithms can enable UAVs to make real-time decisions in complex environments and reach the optimal solution, aiming to meet the mission requirements.

IoT-based UAV networks is a novel emerging field, that combines the UAV network dynamic capabilities with the IoT power. Such solutions can be powerful and highly effective for mission critical services. Cooperation with edge computing can bring additional power of UAV/IoT systems. However, using advanced technologies on sensing, edge computing, computing, and data processing and interpretation, while AI/ML-based, requires further research work of appropriate models, protocols, validation, and also considerations of human-centric global issues (climate, energy, pollution, battlefield, wellness). The advent of AI/ML-based approaches for guiding and orchestrating the interpretation of visual patterns, optimizing path, real-time multi-prong decisions and complex and dynamic systems, led to a powerful triad: AI-IoT-UAV.

This conference was very competitive in its selection process and very well perceived by the international community. As such, it attracted excellent contributions and active participation from all over the world. We were very pleased to receive a large amount of top quality contributions.

We take here the opportunity to warmly thank all the members of the AIVTS 2025 technical program committee as well as the numerous reviewers. The creation of such a broad and high quality conference program would not have been possible without their involvement. We also kindly thank all the authors that dedicated much of their time and efforts to contribute to the AIVTS 2025. We truly believe that thanks to all these efforts, the final conference program consists of top quality contributions.

This event could also not have been a reality without the support of many individuals, organizations and sponsors. We also gratefully thank the members of the AIVTS 2025 organizing committee for their help in handling the logistics and for their work that is making this professional meeting a success.

We hope the AIVTS 2025 was a successful international forum for the exchange of ideas and results between academia and industry and to promote further progress in UAV and IoT research. We

also hope that Barcelona provided a pleasant environment during the conference and everyone saved some time for exploring this beautiful city

AIVTS 2025 Steering Committee

Yasushi Kambayashi, Sanyo-Onoda City University, Japan
Lasse Berntzen, University of South-Eastern Norway, Norway

AIVTS 2025

Committee

AIVTS 2025 Steering Committee

Yasushi Kambayashi, Sanyo-Onoda City University, Japan
Lasse Berntzen, University of South-Eastern Norway, Norway

AIVTS 2025 Technical Program Committee

Mohd Helmy Abd Wahab, Universiti Tun Hussein Onn Malaysia, Malaysia
Sourav Banerjee, Kalyani Government Engineering College, India
Amir Behjat, University at Buffalo, USA
Lasse Berntzen, University of South-Eastern Norway, Norway
Mahdis Bisheban, University of Calgary, Canada
Eugen Borcoci, National University of Science and Technology POLITEHNICA Bucharest, Romania
Daniel Dasig Jr., De La Salle College of Saint Benilde, Manila / College of Professional and Graduate Studies, De La Salle University Dasmarinas, Philippines
Yasushi Kambayashi, Sanyo-Onoda City University, Japan
Constantin Paleologu, National University of Science and Technology POLITEHNICA Bucharest, Romania
Narmeen Shafqat, National University of Sciences and Technology (NUST), Islamabad, Pakistan
K.M. Soni, Amity University, India

Copyright Information

For your reference, this is the text governing the copyright release for material published by IARIA.

The copyright release is a transfer of publication rights, which allows IARIA and its partners to drive the dissemination of the published material. This allows IARIA to give articles increased visibility via distribution, inclusion in libraries, and arrangements for submission to indexes.

I, the undersigned, declare that the article is original, and that I represent the authors of this article in the copyright release matters. If this work has been done as work-for-hire, I have obtained all necessary clearances to execute a copyright release. I hereby irrevocably transfer exclusive copyright for this material to IARIA. I give IARIA permission or reproduce the work in any media format such as, but not limited to, print, digital, or electronic. I give IARIA permission to distribute the materials without restriction to any institutions or individuals. I give IARIA permission to submit the work for inclusion in article repositories as IARIA sees fit.

I, the undersigned, declare that to the best of my knowledge, the article is does not contain libelous or otherwise unlawful contents or invading the right of privacy or infringing on a proprietary right.

Following the copyright release, any circulated version of the article must bear the copyright notice and any header and footer information that IARIA applies to the published article.

IARIA grants royalty-free permission to the authors to disseminate the work, under the above provisions, for any academic, commercial, or industrial use. IARIA grants royalty-free permission to any individuals or institutions to make the article available electronically, online, or in print.

IARIA acknowledges that rights to any algorithm, process, procedure, apparatus, or articles of manufacture remain with the authors and their employers.

I, the undersigned, understand that IARIA will not be liable, in contract, tort (including, without limitation, negligence), pre-contract or other representations (other than fraudulent misrepresentations) or otherwise in connection with the publication of my work.

Exception to the above is made for work-for-hire performed while employed by the government. In that case, copyright to the material remains with the said government. The rightful owners (authors and government entity) grant unlimited and unrestricted permission to IARIA, IARIA's contractors, and IARIA's partners to further distribute the work.

Table of Contents

Design Feasibility and Link Budget Assessment of Aerial 5G IoT and eMBB Connectivity 1
Jyrki T. J. Penttinen

An AI-Powered Aerial Navigation System for Dynamic Accessibility Aware Pathfinding 8
Ayushi Dwivedi and Zahra Derakhshandeh

Design Feasibility and Link Budget Assessment of Aerial 5G IoT and eMBB Connectivity

Jyrki T. J. Penttinen
Alphacore Inc.
Tempe, Arizona, USA
e-mail: jyrki.penttinen@alphacoreinc.com

***Abstract*—Uncrewed Aerial Vehicles (UAVs) equipped with radios can establish rapid, ad-hoc connectivity in areas where terrestrial infrastructure is unavailable or compromised. Leveraging the virtualized architecture of Fifth Generation (5G) mobile networks, both base station and required minimal core functions can be hosted aloft, enabling agile IoT or eMBB centric private networks for emergency response, expeditionary, military operations, and consumer events. This study evaluates the technical feasibility of UAV-mounted 5G Non-Public Network assembled from commercial off-the-shelf components, comparing the physical radio layer performance of IoT and evolved mobile broadband use cases. Candidate 3GPP architectural options are reviewed, and radio link budget calculations quantify physical layer performance in open and rural environments for a single-UAV. The obtained results highlight the trade-off between frequency band, UAV-altitude, and the resulting radio coverage and data rate, providing design guidance for lightweight, energy-efficient aerial 5G systems.**

Keywords-aerial 5G network; link-budget analysis; uncrewed aerial vehicle (UAV); non-public network (NPN); drone-mounted IoT and eMBB radio service; emergency communications; ad-hoc radio access network (RAN).

I. Introduction

Apart from their commercial use, cellular systems can be deployed also as complementing ad-hoc networks, e.g., in emergency solutions after a natural disaster that has damaged telecommunications infrastructure, or in scenarios where non-permanent augmented capacity and radio coverage are desired. A Fifth Generation (5G) private mobile network model through temporally deployed base stations can provide a suitable platform for data transfer and signaling in such situations, enabling enhanced communications and situation awareness also for, e.g., defense groups.

However, in temporal ad-hoc use cases, 5G users may be highly mobile, so deploying terrestrial trailer-mounted radio base stations may not suffice, as the varying link conditions alter quality and can result in uncertainties, resulting in radio network outages when users are on the move. An aerial ad-hoc 5G network that follows the underlying users can provide an important opportunity to overcome these challenges.

3GPP is developing the Internet of Things (IoT) concept further in 5G as a logical continuum from the 4G era, in terms of massive Machine Type Communications (mMTC). 5G IoT in 3GPP is realized through legacy Long-Term Evolution (LTE) -based Narrow-Band IoT (NB-IoT) and LTE for Machines (LTE-M) seamlessly attached to the 5G Core Network (CN) and, from Release 17 onward, through 5G New Radio (NR) RedCap, which is a native, reduced-bandwidth flavor of NR, and evolves further as of Release 18 [1]. Combining Non-Public Network (NPN) and IoT through aerial platform enables novel means to develop and provide low-power, low-data rate services in very large areas.

This paper presents a feasibility study of a UAV-based 5G radio network that can be used in various Line of Sight (LOS) scenarios through 5G NPN. Section II discusses the state-of-the art of UAV-assisted wireless communication and current gaps. Section III presents IoT and eMBB, and Section IV discusses 3GPP-defined 5G NPN. Section V describes a 5G-UAV concept and discusses UAV-mounted equipment, presenting an example of a feasible set. Section VI describes physical radio aspects, and Section VII presents the results obtained for validation of radio network performance applying adequate radio propagation modeling for aerial network, comparing 5G eMBB and IoT use cases that represent two “extremes” in terms of achievable 3D-network coverage areas. Finally, Section VIII summarizes the findings, and Section IX presents the plan for further research.

The novelty of this research lies in the following: 1) it presents a concept based on 3GPP-defined NPN-architecture and available Commercial Off-the-Shelf (COTS) components to provide aerial IoT and data services to a variety of use cases and 2) it evaluates performance of such a solution comparing UAV-mounted 5G gNB performance of eMBB and mMTC.

This study considers single UAV for local communication to a set of User Equipment (UE) underneath, paving the way for the forthcoming work that will consider the formation of a multi-UAV-based 5G RAN service and automized location functions through advanced sensing and artificial intelligence.

II. UAV-Assisted Networking

The global 5G deployments are expanding. The GSM Association (GSMA) estimates that the adaption for 5G will surpass that of 4G in 2028, whereas the earlier networks, 2G and 3G, keep losing their customers; in fact, many of these networks have already been decommissioned [2]. The current 5G system architecture models enable various deployment options and variations for tailored solutions. Examples of these facilitators include new NPN architectures, non-terrestrial networks (NTN), Open RAN, and mMTC, that are evolving and being deployed in commercial networks.

While 5G matures, there are already concrete efforts to develop systems beyond 5G (B5G), paving the way for Sixth

 ISBN: 978-1-68558-317-0

Generation (6G) [3]. During Release 20, 3GPP has carried out use case and feasibility studies, and the actual forming of technical 6G specifications begins along with the Release 21. The first commercial 6G networks can be expected to be available as of 2030 [4]. The 6G is anticipated to be particularly attractive for connected UAVs due to significant improvements, including ubiquitous 3D connectivity on the ground and in the air [5].

While 6G is still under development, the current 5G systems outperform the previous generations, and can be tailored to provide radio service also beyond traditional terrestrial base stations through Service-Based Architecture (SBA) and Service-Based Interfaces (SBI) that handle specific needs of varying use cases and dynamically provide optimal sets of required and available resources to different usage types through Network Functions Virtualization (NFV).

The key benefit of 5G is its ability to run Network Functions (NF) on COTS hardware. This evolution makes 5G a suitable candidate also for UAV-type networking, e.g., through non-public network models as they can form an architectural base for isolation (with augmented security) or interconnection / roaming (providing wider connectivity) network segment. A Mobile Network Operator (MNO) or Network Slice (NS) Provider (NSP) can set up NSs, that can be used for deploying UAV-networks, too.

5G systems can be optimized further through Open RAN (Radio Access Network). Examples of the efforts driving Open RAN include Open RAN Alliance's O-RAN [6] and Telecom Infra Project's TIP [7]. Via Open RAN, vendor-specific internal RAN interfaces are opened so that an extended number of stakeholders can provide select RAN protocol layers independently, increasing efficiency and reducing costs [8], and it can be used also in UAV-based networking [9].

As for the State of the Art and challenges, the mobile networks' radio coverage extension mounting a base station or repeater on aerial vehicle has been studied from several points of view, such as how to maximize the radio coverage by optimal UAV positioning [10] and how to enable group handover for drone base stations [11] related to the mMTC, use of data services, and commercial needs for respective coverage and capacity extension to facilitate adequate data rates and Quality of Service (QoS) for the subscribers.

On radio link budget, there are various studies such as [12] (high-altitude platform for 5G access node) and [13] (system model for forward link transmissions in an Integrated Access and Backhaul IAB multi-tier drone cellular network). An example of real-world UAV-based networking is AT&T's 5G Cell on Wings (CoW), a drone-mounted cellular 4G or 5G base station that temporarily extends radio coverage, e.g., during disasters and large events [14].

Nevertheless, the available studies are not necessarily conclusive in terms of the tradeoffs of the UAV altitude and wider set of deployed frequency bands [15]. Furthermore, the adaptation of optimal architectural models of UAV-networking, considering the feasibility and gaps of COTS components, can benefit from additional research [16].

TABLE I. COMPARISON OF KEY ASPECTS OF 5G EMBB AND IOT

Item	eMBB	IoT
Channel bandwidth	20 – 400 MHz	180 kHz – 20 MHz
SNR (BLER<10%)	8 – 15 dB (64 / 256 QAM)	-13 – -3 dB (BPSK / QPSK, heavy coding)
Fade/penetr. marg.	3 – 5 dB	10 – 15 dB
Device TX power	23 dBm (smartphone)	14 – 23 dBm (sensor)
Data rate target	10 Mb/s – 1 Gb/s	50 b/s – 1 Mb/s

TABLE II. PRIVATE NETWORK TYPES IN UAV-BASED DEPLOYMENTS

Variant	Assessment
SNPN (fully standalone architecture)	Best for autonomous, localized, quick-to-deploy networks (no MNO dependency)
PNI-NPN with radio access network sharing	Enables UAVs to share ground RAN where available, while maintaining separate core
PNI-NPN with core network sharing	UAV-based NPN reuses public 5G core network, allowing leaner deployment
UE route selection via mobile network selection	UEs served by UAVs can select between private and public network profiles

III. IOT VS. EMBB

The 5G eMBB and IoT (mMTC) represent opposites in terms of many aspects, like data rates, power consumption and number of simultaneously communicating devices. These elements dictate also the achievable radio coverage area size. For example, IoT has been optimized for bandwidth given that IoT payloads are small, and narrow band lowers the thermal noise floor. IoT relies on robust modulation schemes and Hybrid Automatic Repeat Request (HARQ) repeats balancing respective throughput and coverage. It is important to note that battery-driven IoT modules stay below 1 W to meet license and life constraints (e.g., NB-IoT Class 3 and Class 5 use 23 dBm and 20 dBm, respectively). Table I summarizes some of the key differences of IoT and eMBB.

IV. AERIAL PRIVATE NETWORK CONSIDERATIONS

3GPP has designed private network realizations through Standalone Non-Public Network (SNPN) and Public Network Integrated Non-Public Network (PNI-NPN) models [17] as presented in Table II. Although 3GPP designed these models for terrestrial networking, their principles can be extended to serve also in aerial networks.

For the architectural modeling of 5G-based UAV network, the following technical specifications form the base: 1) 3GPP TS 23.501 (System Architecture for the 5G System) defines high-level architecture for both SNPNs and PNI-NPNs [18]; 2) 3GPP TS 23.548 (5G System Enhancements for NPN) explores enhancements specific to NPNs (e.g., management, registration, selection) [19]; and 3) 3GPP TS 22.261 (Service Requirements for 5G System) covers typical service-level requirements relevant to NPNs including verticals, e.g., public safety [20] stating also that 5G is expected to support various enhanced UAV scenarios for applications and scenarios for low altitude UAVs in commercial and government sectors.

SNPN is self-contained and independently operated from public networks. It is adequate for rapid deployment for on-

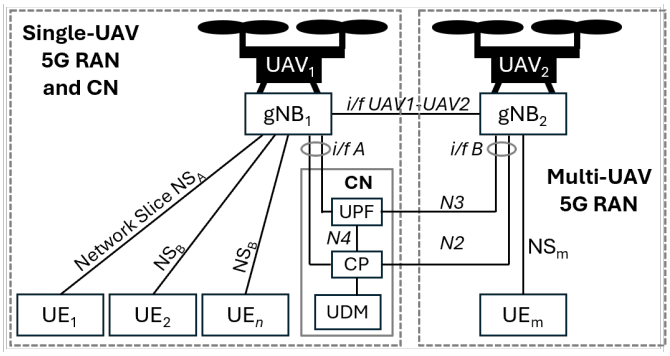

Figure 1. UAV-based, isolated SNPN realization; this feasibility study considers radio performance of a single 5G-UAV scenario

demand aerial networks with no dependency on commercial MNO infrastructure and is thus a match for UAV-based temporal networks serving field units. PNI-NPN, in turn, is an NPN deployed with integration into a public mobile network, and it may share infrastructure (e.g., RAN or core network). The variants of PNI-NPN include RAN-sharing with network slicing, core network sharing; and UEs with public and private subscriptions (PLMN/NSI selection).

Table II summarizes the 3GPP-defined NPN types and presents their key benefits related to their applicability for forming UAV-based network services.

V. 5G-Capable UAV Realization

A. Architecture

The system considered in this study is based on minimal viable 5G SNPN architecture and a single UAV equipped with a 5G gNB (gNode B) enabling local connectivity to the UEs underneath to provide temporarily deployable service if complementing MNO infrastructure is not available. Figure 1 presents the UAV-based SNPN realization in this study. UAV (or set of UAVs) can house radio functions, whereas the essential core network functions of gNBs can be implemented on the same UAVs, separate UAVs, or ground station.

This model can be extended to cover additional UAVs and respective gNBs that are interconnected (e.g., through low-latency PC5 link between vehicles) forming a 5G RAN drone swarm, e.g., via 5G-based mesh between UAVs.

In multi-UAV 5G radio service provisioning, it can be reasoned that maintaining optimal 3D placement is hard as small altitude shifts swing path loss and backhaul Signal-to-Noise Ratio (SNR), so sufficient overlapping must be ensured. Some additional challenges include satellite positioning jitter or denial that can degrade the Time Division Duplex (TDD) timing and node loss fragments control. To overcome these challenges, control can be made hierarchical (central planner and local packet core), and use of multi-source timing can help in this. The rapid geometry changes are another challenge as they may trigger ping-pong handovers, especially in the case of narrow NR beams that raise beam-failure risk in UAV turns. Also, a dominating cell with a weak multi-hop backhaul can impact negatively the Quality of Service (QoS).

TABLE III. Functional architecture of aerial 5G system

Layer	Function	Realization
Radio Access (RA)	gNB (5G standalone) with full UE-to-UE routing support	Lightweight COTS integrated into small cell
Control Plane (CP)	Lightweight distributed UAV logic (also swarm consensus)	Simple microcontroller and onboard logic
Backhaul (BH)	None (fully isolated); direct local P2P 5G	PC5 direct-mode or local user plane function (UPF)
Intelligence	Initially manual; advanced version has UE-following	Position, RSSI-based positioning heuristics
UE Signaling	Simple beaconing uplink from UEs, e.g., by Synchronization Signal Blocks (SSBs)	Existing 5G UE support
Swarm Comms	When more than one UAV, 5G-based mesh between UAVs	5G PC5 (Sidelink)

TABLE IV. Examples of 5G RAN key equipment per UAV (*power consumption estimated in typical average / peak watts)

Component	Description	Example	Weight	Power*
Integrated 5G Small Cell	Embedded gNB; RU (SA mode)	Amarisoft Callbox Mini / Baicells Nova430	400 – 800g	25 / 40W
Light Compute Module	For basic UAV / swarm logic	Raspberry Pi CM4 or Jetson Nano	100 – 200g	8 / 12W
Simple Mesh Swarm Radio	IEEE 802.11s Wi-Fi 6 / V2V PC5	Compex WLE900VX / 5G module	50 – 100g	6 / 12W
Battery Pack	Standard UAV LiPo	6S 22000 mAh	1.5 – 2.0kg	0.6 / 1W
Positioning Sensors	GPS, IMU	COTS GPS + Pixhawk FC	<100g	3 / 5W

To overcome this challenge, it is possible to apply larger handover hysteresis (e.g., 3-5 dB) and time to trigger (e.g., 160-320 ms), implement dual connectivity feature (make-before-break), and use backhaul-weighted cell selection.

B. Equipment Considerations

To deploy a 5G SNPN UAV RAN, the UAV can host a basic integrated gNB (e.g., Amarisoft / Parallel Wireless). The basic location management is assumed to be manual and satellite positioning system -assisted, but automated methods can also be developed based on UE signals and using basic Radio Frequency (RF) heuristics (e.g., weighting received signal strength indicator) to position the UAV(s) according to user density.

Basing the solution on COTS devices, Table III presents a set of feasible candidate elements for simplified functional architecture.

Table IV presents examples of UAV-mounted equipment. For advanced alignment of the UAVs and UEs, downward-facing cameras can be considered for UE clustering estimation (COTS-based image processing) and barometers for altitude stabilization. Based on the selected options minimizing the weight of the components, the total UAV payload (essential RAN components) is at minimum approximately 2.5–3.0 kg, which is feasible for medium-class UAVs (e.g., DJI Matrice 300 RTK [21] or similar custom UAVs).

One of the key challenges of UAV-based networking is the limitations of power supply, which represents the major weight of the payload. As an example, the above-mentioned DJI Matrice 300 RTK supports up to 55 minutes operational flight time [21]. For the communication components, Table IV presents a rough estimate of the average and peak power drain. As can be seen, the gNB consumes major part of the total power. For the operational power of the UAVs and 5G RAN components, this feasibility study assumes ideal power management, but in practice, hybrid model can be used with tethered UAVs (permanent anchor nodes with gNBs) and rotating UAVs (fly, recharge, rotate). Complementary power sources can be, e.g., solar panels (small flexible panels on UAV structure extending flight by approximately 10-20%), hydrogen fuel cells (about 2-3× endurance of lithium polymer, LiPo), or tethered power supply forming wired UAVs with unlimited power (for anchor UAVs [22]).

It should be noted that regulation limits the operational boundaries in terms of UAV altitude and maximum radiated power. As an example, there is no general airborne-gNB EIRP allowance in the USA and the power is what the experimental or carrier's license and service rules permit, often with tight coordination to prevent wide-area interference. US-rules dictate 400 ft for the maximum UAV altitude above ground level (AGL) under Part 107, although higher values can be permitted via waiver. In the EU, routine airborne gNBs are not covered by the standard local/private-5G licenses, so specific or certified flight approval is needed with EASA framework as well as a trial or temporary spectrum license from the national regulator, and the maximum altitude is 120 m AGL.

VI. Physical Radio Interface

This feasibility study considers theoretical coverage limits of a single UAV applying relevant propagation loss models, with the aim to provide optimal 5G RAN quality and performance as a function of UAV altitude (and later, inter-UAV distance) in rural and open areas, and the following parameters: 1) Frequency band f = low (1 GHz), mid (3.5 and 6 GHz) and high (24 and 28 GHz); 2) UAV altitude h_{gNB} = 50m, 100m,. . . , 400m; 3) UE type = pedestrian; 4) Power = P_{UE} +23 dBm, P_{gNB} +23 dBm; 5) UAV antenna type = omni-directional (0 dBi gain, uniform, ideal radiation pattern). The key results include achievable cell size and respective data rate estimate for both eMBB and IoT use cases.

The starting point of the study was to consider a single UAV that houses 5G SNPN equipment needed to form basic radio access for the UE-UAV$_{\text{gNB}}$-UE communications.

In rural and open-space areas, for the line of sight (LOS) scenarios, the free space path loss L_{FSPL} (in dB) can be estimated by applying the ITU-R P.525 model (within version 12 of ITU-R P.1411) that assumes minimal obstructions [23]. The LOS path loss equation is:

$$L_{FSPL} = 20log_{10}f + 20log_{10}d + 92.45 \quad (1)$$

In this equation, f is the frequency in GHz and d is the distance in kilometers between UAVgNB and UE.

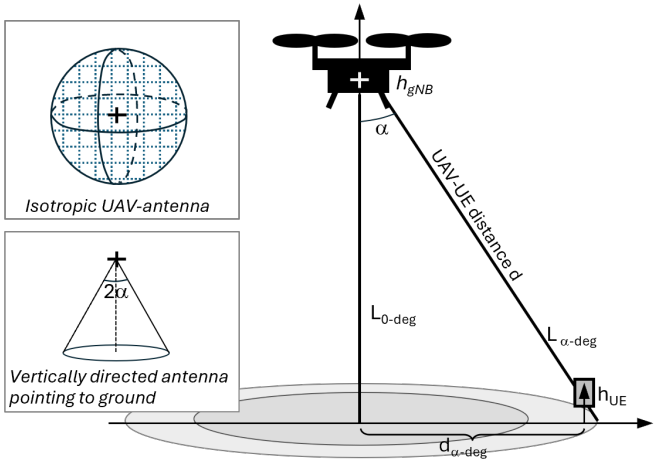

Figure 2. Principle of (theoretic) radiation patterns and respective radio coverage formation assumed in this study

In the feasibility study presented in this paper, Figure 2 depicts the principle of the UAV setup. For the baseline and comparative reference, this study is based on a theoretical omnidirectional UAV-mounted 0 dBi antenna. In practice, isotropic antenna gain is conservative whereas directive antenna enhances the link and optimizes the radio coverage also for minimizing the interference; an example of this is a cone-shaped vertical radiation pattern as depicted in Figure 2. In field deployments, an adaptive Multiple-In Multiple Out (MIMO) antenna provides augmented performance, capacity, and interference mitigation, but the drawback is the increased complexity and power consumption. To keep the antenna complexity and respective power consumption at minimum in this study, passive omni-directional approach provides means to materialize multi-UAV gNB connectivity without a need for a specific steering logic. In practice, for the final selection of the antenna type and respective gain, detailed radio network planning is important for ensuring adequate inter-UAV connectivity and radio cell dimensioning. The impact of the final antenna gain can be considered adjusting the presented GTX parameter values.

VII. Results

Using ITU-R P.1411, Figure 3 presents the path loss UE-UAV at a distance d from UAV's location for isotropic UAV TX antenna at 100 m altitude (earth curvature limit 35 km) for frequency bands 1 GHz – 28 GHz.

Considering the same frequency range 1 GHz – 28 GHz, Figure 4 summarizes the estimated path loss values L (dB) directly beneath (a=0º) and off the vertical location of the UAV (a=30º) in open and rural areas, when the UAV altitude varies between 50 m and 400 m. The presented LOS path-loss estimates show that the altitude-distance trends for 1–28 GHz match the 3GPP TR 38.901 LOS baseline [24]. Comparable UAV-gNB studies at 28 GHz [25] [12] show the same free-space path loss driven scaling, with practical shortfalls mainly from blockage, beam-pointing, and backhaul constraints rather

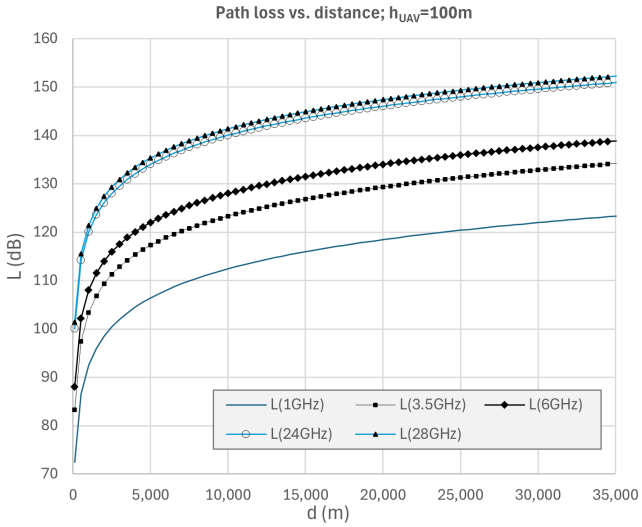

Figure 3. Path loss of UAV-UE as a function of the UE's distance from UAV's vertical reference location (UAV altitude is 100m)

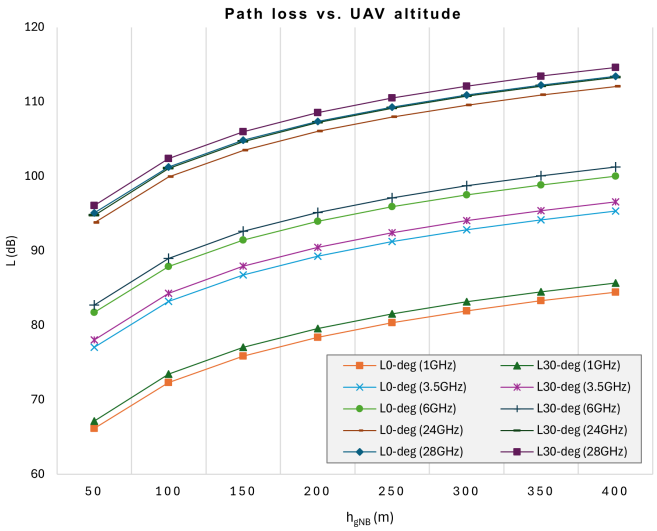

Figure 4. Path loss prediction, 1GHz–28GHz, for UAV altitudes of 50m–400m

than the LOS model itself. Consistent with geometry, off-nadir (30°) incurs about 1.25 dB extra loss from the longer slant range, and at 100 m altitude the footprint is curvature-limited. Deployment planning can thus start with FSPL-based bounds and subtract environment-specific losses for realistic coverage.

A. Scenario: eMBB

Table V presents the key eMBB radio budget items, and Table VI presents an example of the radio link budget when the UAV altitude is 400 m and the UE is located underneath.

In these scenarios, the channel bandwidth is 20 MHz (1 GHz), 100 MHz (3.5/6 GHz), or 400 MHz (24/28 GHz). In these calculations, spectral efficiency model is η (bps/Hz) = $0.6\times\log_2(1+\text{SNR})$. The assumption for the 0.6 factor is due to scheduler, modulator and coding inefficiencies that lower

TABLE V. APPLIED RADIO LINK BUDGET ITEMS, EMBB SCENARIO

Parameter	Value	Notes
gNB transmitter power P_{TX}	+23 dBm	Typical small-cell power limit, applicable to a UAV-mounted gNB
TX antenna gain G_{TX}	0 dBi	Isotropic (no beamforming)
UE antenna gain G_{RX}	0 dBi	Smartphone baseline
Fade margin M	3 dB	Covers body loss, ageing, fading
UE noise figure NF	7 dB	5G NR handset typical
Thermal noise density	–174 dBm/Hz	$N_o=kT=1.38\times10^{-23}$ J/K × 290K

TABLE VI. EXAMPLE OF THE RADIO LINK BUDGET (D=400M)

Link budget, h_{UAV}=400m, α=0°	**1 GHz**	**3.5 GHz**	**6 GHz**	**24 GHz**	**28 GHz**
Path loss PL, dB at (2km)	84.5	95.4	100.1	112.1	113.4
Tx power (gNB), dBm	23.0	23.0	23.0	23.0	23.0
Tx antenna gain, dB	0.0	0.0	0.0	0.0	0.0
UE antenna gain, dBi	0.0	0.0	0.0	0.0	0.0
Implementation/fade margin, dB	3.0	3.0	3.0	3.0	3.0
UE noise figure NF, dB	7.0	7.0	7.0	7.0	7.0
Thermal noise density, dBm/Hz	-174	-174	-174	-174	-174
Channel bandwidth, MHz	20	100	100	400	400
Received power Prx, dBm	-61.5	-72.4	-77.1	-89.1	-90.4
Noise floor N, dB	-94.0	-87.0	-87.0	-81.0	-81.0
Operational SNR after margin, dB	29.5	11.6	6.9	-11.1	-12.5
Spectral efficiency SE	5.88	2.38	1.54	0.06	0.05
Data rate, Mb/s	**117.6**	**237.5**	**154.4**	**25.8**	**19.1**

the theoretic capacity of Shannon limit. The received power is $P_{RX} = P_{TX} + G_{TX} + G_{RX} - L$, and the noise floor is $N = -174 + 10\log_{10}B + NF$. The operational signal to noise ratio (SNR) after margin is $\text{SNR} = P_{RX} - N - M$. The spectral efficiency $SE = 0.6\times\log_2(1+10^{\text{SNR}/10})$, and the data rate is $R = SE \times B$. Beyond the presented calculations, the effective SINR enhances through beamforming gain G_{BF} that is typically 3-10 dB whilst the level of interference lowers it respectively. MIMO, in turn, adds rank often 1-2 aloft scaling efficiency, and resource allocation gives a per-UE share 0.3-0.8. [26]

Figure 5 and Figure 6 summarize the impact of h_{UAV} (50 m – 400 m) on the received single user data rate considering the space below the UAV and surrounding region. The results are based on analytical modeling of path loss prediction and a set of radio link budget attribute values (select examples presented in Table V and Table VI), varying the UAV altitude.

As can be seen, high-band (24 GHz and 28 GHz) provides the highest rates when the distance between UAV_{gNB} and UE is relatively short, but the rate lowers drastically as the distance between UAV and UE increases over a few hundred meters due to the strong attenuation of this band. As can be expected, the mid-band (3.5 GHz and 6 GHz) performs more constantly at short distances and nearby regions.

Taking a closer look at the short distance (5–200 m) between

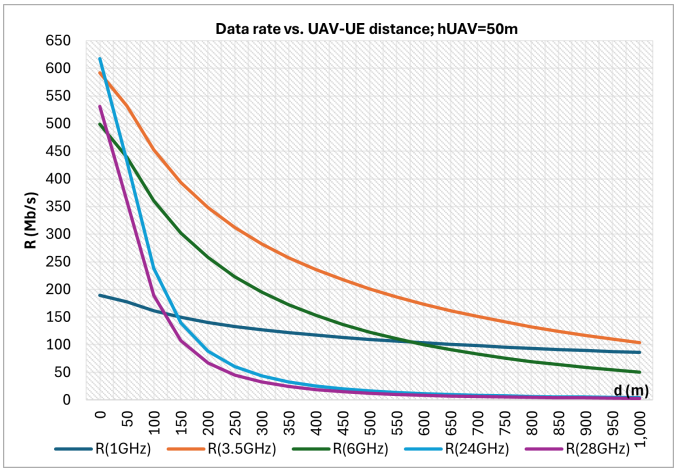

Figure 5. Data rate for UAV-mounted 5G gNB at 50 m altitude

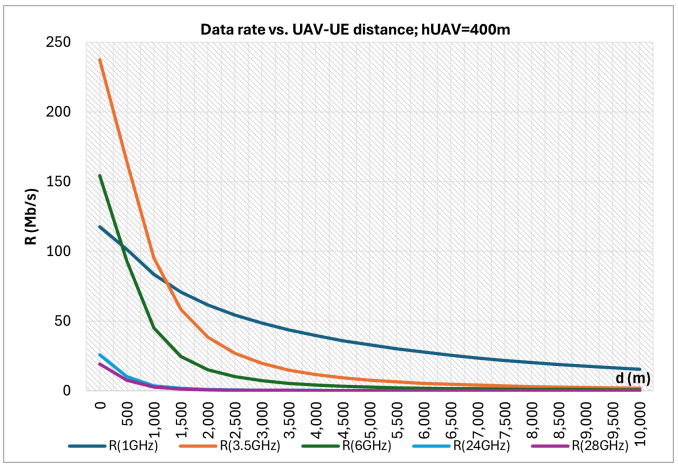

Figure 6. Data rate for UAV-mounted 5G gNB at 400 m altitude

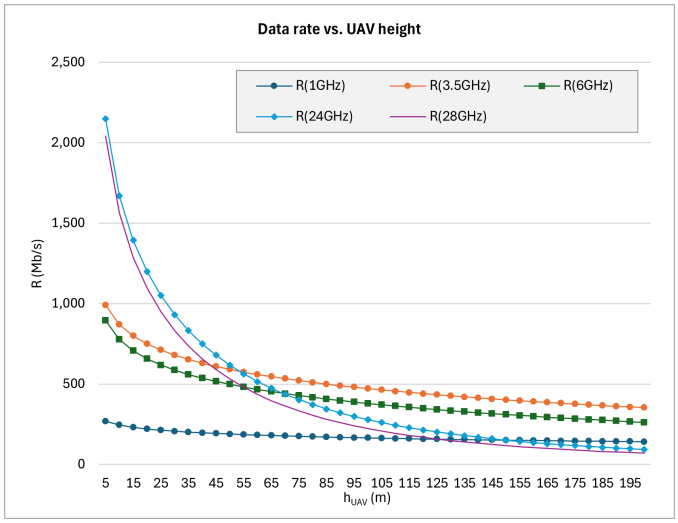

Figure 7. Data rate behavior when the distance between the UAV and UE is short (5-200m)

TABLE VII. APPLIED RADIO LINK BUDGET ITEMS, IOT

Link budget	**NB-IoT$_{CE0}$**	**NB-IoT$_{CE2}$**	**LTE-M**	**Red Cap**
Channel bandwidth, MHz	0.18	0.18	1.40	5.00
Thermal noise floor, dBm	-114.4	-114.4	-105.5	-100.0
Impl. / fade margin, dB	8.0	14.0	8.0	5.0
Required SNR / E_b/N_o	-5.0	-13.0	-7.0	-3.0
RX sensitivity, dBm	-119.4	-127.4	-112.5	-103.0
Peak data rate, b/s	25k	50-100	1M	150M
Path loss budget, dB	**134.4**	**136.4**	**127.5**	**121.0**
Distance (1GHz), km	»35	»35	»35	~25
Distance (3.5GHz), km	~35	>35	~15	~7

the UAV and UE, Figure 7 shows more detailed behavior. As can be seen, high-band outperforms the other bands up to about 50 m distances providing 1–2 Gb/s data rates, but afterwards, mid-band provides the highest rate (250–500 Mb/s). The heavy attenuation of the high-band makes also the low-band data outperform it beyond 150–200 m distance.

Figure 7 shows that for a critical mission in open and rural areas; if the key requirement is fast data connectivity and high capacity, e.g., for high-definition video contents, high-band provides the most performant service up to about 100 m.

If, instead, the main requirement is a large coverage area (e.g., over 10 km), and the UAV operation is possible at high altitude (e.g., 400 m), low-band is adequate selection as Figure 6 indicates. Should there be limitations for the UAV altitude, such as nearby airports or other restricted areas, mid-band (particularly 3.5 GHz) provides the most adequate balance for h_{UAV} and radio performance, as can be seen in Figure 5.

B. Scenario: IoT

Table VII presents key radio budget items for the IoT scenario comparing NB-IoT class CE0 and CE2, LTE-M, and RedCap.

In all these cases, the gNB transmitter power is 23 dBm, TX and RX antenna gains are 0 dBi, and RX noise figure is 7 dB (typical low-cost IoT modem). Again, the free-space path loss model is used in these calculations. Receiver sensitivity is driven by bandwidth, i.e., noise floor plus the required SNR for the lowest modulation / coding of each profile. Path-loss budget is the maximum loss the link can tolerate after allocating the fade / implementation margin. Converting that budget to free-space distance shows the theoretical cell radius; real-world coverage will be smaller due to UAV altitude (earth curvature), foliage, buildings and interference. The presented SNR / (E_b/N_0) values are for the lowest-order modulation / coding in each profile (reference sensitivity) as per the UE RF specifications [27] [28], and the RX sensitivity is *N* + Required SNR (cross-checked with the specifications for minimum guaranteed UE sensitivity).

As can be seen, NB-IoT can reach the radio horizon even with only 23 dBm EIRP; coverage is limited by geometry, not RF. LTE-M at 1 GHz still covers tens of kilometers, whereas at 3.5 GHz it shrinks to about 15 km LOS. NR RedCap offers the highest data rates but requires roughly 10 dB more SNR than NB-IoT, confining its cell to single-digit-kilometer radii at 3.5 GHz. These tables can be used directly to size UAV altitude, antenna gain, or additional power needed for a given IoT service profile. Compared with the broadband case (for

which MCL is 95–105 dB), IoT enjoys tens of dB link budget head-room mainly from the narrow bandwidth and low SNR requirement. Thus, all the presented IoT cases outperform the radio coverage of the eMBB.

VIII. Summary

This study demonstrates that a single-UAV 5G SNPN assembled from COTS components can furnish rapid, standards-based connectivity for both eMBB and IoT use cases in open and rural terrain. Using the ITU-R P.1411 LOS formulation as the baseline propagation model, we quantified how frequency (1–28 GHz) and UAV altitude (50–400 m) shape the coverage–throughput trade-space. The altitude–distance trends and off-nadir penalties are FSPL-driven, with the 100 m footprint ultimately curvature-limited, while mmWave bands deliver the highest short-range rates but degrade fastest with distance. In contrast, mid-band (3.5–6 GHz) offers robust, meter-to-kilometer performance, and low-band (1 GHz) maximizes area at higher altitudes.

Link-budget templates for eMBB and IoT profiles show IoT's tens-of-dB margin advantage from narrow bandwidths and low required SNR, often making coverage geometry-limited instead of RF-limited. Practicality is supported by a lightweight payload bill where the gNB dominates power, informing endurance planning.

Noting regulatory envelopes and spectrum authorization constraints, the results indicate that UAV-based 5G NPN deployment should select band and altitude by required rate vs. area, start with FSPL bounds and subtract environment-specific excess loss, and budget power and weight for the radio. These results provide actionable sizing baselines for future study of multi-UAV extensions and AI-assisted placement.

IX. Future Research

The next step in this study will cover 5G-UAV RAN performance evaluation in expanded terrain types, including low- and high-rise urban topologies, applying up-to-date radio propagation models. The future study also considers extended UAV-based RAN network formation through a drone swarm and will evaluate feasible methods for inter-connected gNBs, including AI-assisted coordination. Future research also considers ways to deploy automated positioning functions for the 5G-UAV network with the underneath UEs for which AI may provide feasible means also in presence of interferences, through advanced sensing techniques.

Acknowledgement

I gratefully acknowledge the feedback of Professors M. Reisslein, G. Trichopoulos, S. Zeinolabedinzadeh, and A. Alkhateeb of Arizona State University on this work.

References

[1] 3GPP, "TR 38.865: Study on further NR RedCap UE complexity reduction," 2022.

[2] GSMA, "Mobile economy report 2025," GSMA Intelligence, London, UK, 2025.

[3] J. Penttinen, "On 6G visions and requirements," Journal of ICT Standardization, vol. 9, no. 3, pp. 311-325, 2021.

[4] P. Jain, "3GPP SA 6G planning and progress," 3GPP, 2024.

[5] G. Wikstrom and S. Thorson, "Explore the impact of 6G," Ericsson, 19 December 2024. [Online]. Available: https://www.ericsson.com/en/blog/2024/12/explore-the-impact-of-6g-top-use-cases-you-need-to-know. [Retrieved 29 August 2025].

[6] O-RAN Alliance, "Who we are," [Online]. Available: https://www.o-ran.org/who-we-are. [Retrieved 29 August 2025].

[7] Telecom Infra Project, "How TIP Works," [Online]. Available: https://telecominfraproject.com/how-we-work/. [Retrieved 29 August 2025].

[8] Ericsson, "Industrializing Open RAN," [Online]. Available: https://www.ericsson.com/en/openness-innovation/open-ran-explained. [Retrieved 29 August 2025].

[9] M. Mushi et al., "Open RAN testbeds with controlled air mobility," Computer Communications, vol. 228, Article 107955, 2024.

[10] M. Saym, M. Mahbub and F. Ahmed, "Coverage maximization by optimal positioning and transmission planning for UAV-assisted wireless communications," in International Conference on Science & Contemporary Technologies (ICSCT), Dhaka, Bangladesh, pp. 294-297, 2021.

[11] Y. Aydin, G. Karabulut, E. Ozdemir and H. Yanikomeroglu, "Group handover for drone base stations," IEEE Internet of Things Journal, vol. 8, no. 18, pp. 13876-13887, 2021.

[12] M. Alamgir and B. Kelley, "Fixed Wing UAV-based Non-Terrestrial Networks for 5G millimeter wave Connected Vehicles," in IEEE 13th Annual Computing and Communication Workshop and Conference (CCWC), pp. 1167-1173, 2023.

[13] A. Fouda, A. Ibrahim and I. Guvenc, "UAV-Based in-band Integrated Access and Backhaul," in IEEE 88th Vehicular Technology Conference (VTC-Fall), Chicago, IL, USA, pp. 1-5, 2018.

[14] S. Howe, "ATT's flying COW transmits 5G network by tethered drone," Commercial UAV News, 29 June 2022. [Online]. Available: https://www.commercialuavnews.com/public-safety/at-t-s-flying-cow-transmits-5g-network-by-tethered-drone. [Retrieved 29 August 2025].

[15] N. Tafintsev, A. Chiumento, O. Vikhrova, M. Valkama and S. Andreev, "Utilization of UAVs as flying base stations in urban environments," in 15th International Congress on Ultra Modern Telecommunications and Control Systems and Workshops (ICUMT), Ghent, Belgium, pp. 7-11, 2023.

[16] P. Valente, A. Teixeira, M. Luis, D. Raposo, P. Rito and S. Sargento, "Easy to deploy UAV-based non-public open-source 5G network," in 15th International Conference on Network of the Future (NoF 2024), Barcelona, Spain, pp. 72-80, 2024.

[17] J. Penttinen, J. Collin and J. Pellikka, "On Techno-Economic Optimization of Non-Public Networks for Industrial 5G Applications," in The Nineteenth Advanced International Conference on Telecommunications (AICT 2023), Nice, France, pp. 1-7, 2023.

[18] 3GPP, "TS 23.501: System architecture for the 5G System (5GS)," 2025.

[19] 3GPP, "TS 23.548: 5G System Enhancements for Edge Computing; Stage 2," 2025.

[20] 3GPP, "TS 22.261: Service requirements for the 5G system," 2025.

[21] DJI, "Support for Matrice 300 RTK," [Online]. Available: https://www.dji.com/support/product/matrice-300. [Retrieved 29 August 2025].

[22] "Drone power feed through ground tethering," 17 April 2025. [Online]. Available: https://yle.fi/a/74-20156841. [Retrieved 29 August 2025].

[23] ITU, "Recommendation P.1411-12 (08/2023)," ITU-R, August 2023. [Online]. Available: https://www.itu.int/rec/R-REC-P.1411-12-202308-I/en. [Retrieved 29 August 2025].

[24] 3GPP, "TR 38.901: Study on channel model for frequencies from 0.5 to 100 GHz (Release 19)," 2025.

[25] M. Gapeyenko, I. Bor-Yaliniz, S. Andreev, H. Yanikomeroglu and Y. Koucheryavy, "Effects of Blockage in Deploying mmWave Drone Base Stations for 5G Networks and Beyond," in IEEE International Conference on Communications Workshops, ICC, Kansas City, MO, USA, pp. 1-6, 2018.

[26] 3GPP, "TS 38.214 (V19.0): NR physical layer procedures for data (Release 19)," 2025.

[27] 3GPP, "TS 36.141: E-UTRA; Base Station conformance testing," 2025.

[28] 3GPP, "TS 36.101: E-UTRA; User Equipment radio transmission and reception," 2025.

An AI-Powered Aerial Navigation System for Dynamic Accessibility Aware Pathfinding

Ayushi Dwivedi
Department of Computer Science
California State University, East Bay
Hayward, USA
e-mail: adwivedi@horizon.csueastbay.edu

Zahra Derakhshandeh
Department of Computer Science
California State University, East Bay
Hayward, USA
e-mail: zahra.derakhshandeh@csueastbay.edu

***Abstract*—Navigating indoor environments brings significant challenges for individuals with mobility impairments, such as wheelchair users, older adults, those with temporary injuries, and others requiring accessible pathways. A key barrier is the absence of reliable, real-time information about indoor layouts, accessibility features, and temporary obstacles. Existing navigation solutions often rely on static maps and outdated data, limiting their ability to address the dynamic and specific needs of users seeking accessible routes. To overcome these limitations, this study introduces an Artificial Intelligence (AI)-assisted drone-based navigation system that provides real-time guidance and adaptive support for individuals with mobility restrictions. We developed and integrated a custom object detection model into the aerial platform to identify accessibility features and environmental obstacles. In addition, a dynamic path-planning algorithm enables the drone to autonomously guide users through accessible routes, adjusting in real-time to environmental changes. The system reroutes users when unexpected obstructions arise, ensuring uninterrupted and reliable navigation to the targeted destination. We evaluated the system's performance through experiments in a controlled environment, demonstrating its effectiveness and potential for real-world applications.**

Keywords-Unmanned Aerial Vehicles; Drone-as-a-Service; Artificial Intelligence; Accessibility; Mobility Impairment.

I. INTRODUCTION

Navigating indoor environments poses challenges for many individuals; however, these difficulties are significantly intensified for those with mobility impairments, including wheelchair users, the elderly, and others requiring accessible pathways. Unlike outdoor environments, which might benefit from widely adopted GPS-based navigation systems, indoor spaces, such as office buildings, shopping malls, hospitals, and airports, are often complex, dynamic, and poorly documented. People with mobility limitations face barriers such as stairs, narrow corridors, inconveniently placed ramps, surface defects, and obstacles that change frequently due to construction, furniture rearrangements, or crowded conditions. They often have to rely on pre-researched maps, verbal directions, or external assistance. In emergencies, timely access to accessible paths can be critical, yet existing systems rarely provide the real-time guidance needed to navigate these spaces safely.

Although considerable progress has been made in accessibility-aware tools and standards for outdoor navigation, indoor environments remain largely unsupported in terms of real-time navigational assistance. People with disabilities often encounter inaccurate, outdated, or difficult-to-access information about accessible paths, ramps, elevators, and temporary obstructions. The cognitive load required to process such information adds to the stress of independent navigation, creating a substantial barrier to mobility, autonomy, and inclusion.

Tools like Google Maps' Accessible Places feature provide high-level accessibility data, but lack support for dynamic rerouting or detection of temporary obstacles. These gaps intensify the urgent need for solutions that can provide adaptive, real-time indoor navigation responsive to users' accessibility requirements.

Recent advances in robotics and Artificial Intelligence (AI) offer promising paths for addressing aforementioned challenges. Unmanned Aerial Vehicles (UAVs), commonly known as drones, have demonstrated broad utility in domains, such as agriculture, surveillance, emergency response, and delivery services. Integrating drones with computer vision and deep learning can enable real-time detection of environmental features and obstacles, while also supporting dynamic path planning. This capability is particularly relevant for indoor environments, where static maps are insufficient, and routes may need continuous updating in response to environmental changes.

Despite these advances, most existing drone-based or AI-assisted navigation systems focus on outdoor applications or visually impaired users, leaving a critical gap for mobility-impaired populations in indoor spaces. There is a need for systems that combine accessibility-aware planning, real-time perception, and reliable guidance to ensure users can navigate complex indoor environments independently or with minimum of help.

In this study, we present a novel AI-assisted drone-based navigation system designed specifically for real-time operation in dynamic indoor environments. Our platform combines a custom object detection model, capable of recognizing accessibility features and obstacles, with a real-time path planning algorithm that prioritizes accessible and safe routing. Unlike previous approaches that rely on pre-recorded routes or static maps, our system continuously adapts its path in response to environmental changes, offering an adaptive navigation experience. The contributions of this paper is as follows:

1. **A practical architecture for drone-assisted indoor navigation** that supports real-time accessibility-aware

guidance.

2. **Integration of AI-based object detection with dynamic path planning** to identify and respond to temporary obstacles, changing layouts, and accessibility features.
3. **Experimental evaluation in controlled indoor environments** demonstrating feasibility and potential to improve independent mobility.
4. **A roadmap for future enhancements**, including dataset and training improvements, integration of crowdsourced annotations, and broader validation across varied indoor environments.

By advancing the convergence of AI, robotics, and accessibility, our system introduces a novel and adaptable solution to a longstanding problem in inclusive navigation. It demonstrates the potential of drones to serve as mobile, intelligent guides, ensuring safe, accessible, and efficient indoor mobility for individuals with physical disabilities.

This paper is structured as follows: Section II reviews related work on accessibilty systems, path navigation, and drone-assisted guidance. Section III introduces the overall system architecture. Section IV, describes the object detection process, including the algorithm, the steps used to identify accessibility features and obstacles, and the corresponding performance results. Section V presents our dynamic path navigation algorithm, which guides users along accessible routes by using real-time environmental data, followed by an anlysis of its complexity and completeness. Finally, Section VI summarizes the contributions and outlines directions for future work.

II. Related Work

A wide body of research emphasizes the limitations of current systems in addressing the needs of people with disabilities indoors. Studies have documented the challenges faced by blind users, including poor signage and misaligned digital-physical information [1], as well as the cognitive load involved in navigating unfamiliar spaces [2]. Other work has examined mobile applications and assistive technologies for people with visual or cognitive impairments [3][4]. However, relatively little attention has been given to real-time, assistive indoor navigation for those with mobility-related impairments. The work [5] on mobile indoor navigation assistance for mobility impaired people proposes a smartphone-based system using Wi-Fi localization and pre-mapped accessibility data to guide users indoors, focusing on using accessible maps and wireless sensor positioning to guide users through complex indoor spaces. While effective for static environments, it lacks dynamic perception and real-time path adaptation. Rafful et al. [6] describes the role of simulation frameworks in assessing indoor accessibility for people with disabilities. While such tools are valuable for design-time evaluation, they do not provide in-the-moment guidance for users moving through an indoor environment. As a result, People With Mobility Disabilities (PWMD) are often left without timely information when routes become blocked or when layouts change.

Issues, such as misalignment between maps and real-world landmarks, uneven terrain, inaccessible detours, and poorly placed signage make independent travel difficult. These obstacles are further worsened by the mental effort required to process complex way-finding information, often turning navigation into a stressful and unreliable task. In emergencies, the situation becomes even more critical, as the absence of real-time navigation support can lead to dangerous delays and confusion. Studies like [7][8] demonstrate the limitations of static maps or pre-fed navigation systems, which often fail to provide the real-time updates needed to address dynamic changes in the environment, such as construction work, temporary obstacles, or crowded areas. Moreover, people with disabilities may hesitate to disclose their conditions or seek assistance, further emphasizing the need for inclusive and adaptive technological solutions.

Some researchers have explored computer vision and deep learning for assistive navigation. For example, Nasralla et al. [9] recommend that researchers use deep learning and machine vision for hazard detection, offering audio or tactile feedback to assist visually impaired users. Khemmar et al. [10] emphasize the potential of deep learning algorithms for robust pedestrian detection and target tracking in dynamic settings. While promising, these solutions focus primarily on outdoor environments or visually impaired users, leaving gaps in addressing indoor navigation for people with mobility impairments.

One promising but underexplored path is the use of drones for indoor navigation. Their proven effectiveness in infrastructure inspection, environmental monitoring, and emergency response indicates their potential to support accessibility-focused applications. The introduction of commercial services like Amazon's drone delivery [11] has fueled public interest and innovation in the field. With the global drone market projected to grow from $15.9 billion in 2023 to $53.4 billion by 2030 [12], the supporting technologies for real-time indoor drone navigation, such as object detection and obstacle avoidance, are increasingly accessible.

Recent studies have explored drones as guides or assistive agents for people with disabilities. For instance, Avila et. al. [13] explore the use of drones to assist visually impaired individuals in navigating public spaces, relying on auditory cues and airflow produced by the drones. The drones follow pre-recorded paths mapped by a sighted individual. Iuga et al. [14] combine wearable fall detectors with drone-based response systems for emergency scenarios. Their system features a fall detection device, worn on the upper arm, which monitors heart rate and detects falls. Upon detecting a fall, the system autonomously dispatches a UAV carrying a first aid package to the patient's location, with the UAV's route planned through a smartphone-based application at an emergency call center. In [15], the authors propose a system that integrates Virtual Reality (VR) with drones to deliver engaging visual experiences for individuals with limited mobility. By streaming live video from the drone's onboard camera to the VR headset, users can experience remote environments in real-

time, effectively bringing the outside world to those unable to physically explore it. While these applications are innovative, they do not directly address real-time indoor navigation for individuals with mobility impairments.

Our work introduces a novel drone-based navigation system designed to assist people with mobility impairments in real-time, dynamic indoor environments. Unlike approaches that rely on pre-recorded routes or fixed maps, our system suggests active detection of key features of the environment, including ramps, stairs, elevators, and obstacles, and continuously updates its planned route as conditions change. The platform integrates an object detection model to identify accessibility features and obstacles in real time, with a real-time path planning algorithm that selects accessible and safe routes for the user. This combination enables the drone to act as a dynamic guide, leading users through the environment while responding to layout changes, temporary obstructions, or changing accessibility conditions.

Effective path planning is critical for any navigation system, particularly for assistive technologies utilizing drones. Research on safety-focused path planning and genetic algorithm-based approaches provide insights into optimal route selection and efficiency [16][17]. In [16], Castelli et al. concentrate on the importance of incorporating safety metrics to enhance reliability during UAV missions. Their method prioritizes minimizing risk by accounting for potential hazards in the operating area, particularly suited for outdoor environments, such as urban areas or disaster zones, where UAVs face dynamic, unpredictable conditions. The study discusses the importance of incorporating safety metrics to enhance reliability during UAV missions. Wang et al. introduced a path-planning method based on genetic algorithms, focusing on outdoor UAV applications [17]. The study is tailored for scenarios requiring efficient and adaptive route selection, such as search and rescue operations, environmental monitoring, and agricultural surveying. This method uses evolutionary computation to optimize UAV paths with multiple objectives, including minimizing energy consumption, avoiding obstacles, and reducing flight time. Genetic algorithms iteratively refine candidate paths, balancing trade-offs between efficiency and safety. Although these approaches demonstrate robust path planning in general settings, they are not designed with accessibility in mind. Our contribution lies in designing a path planning algorithm while prioritizing accessible features and user needs, enabling drones to serve as mobile assistive agents within real-world indoor spaces.

In this article, we address a critical and underexplored gap at the intersection of artificial intelligence, accessibility, and robotics. By integrating real-time object detection and accessibility-aware path planning into a Drone-as-a-Service (DaaS) platform, we aim to support independent mobility of people with physical disabilities in indoor environments that are often inaccessible, unpredictable, or hazardous. Our system offers an adaptable, intelligent, and practical solution to a longstanding problem in inclusive navigation technology. Although the primary focus of this work is not on drone safety concerns, such as the risk of drones falling onto individuals, we acknowledge this as an important practical consideration. One straightforward mitigation strategy involves installing a transparent, glass-like barrier or protective netting below the ceiling, allowing drones to operate above it. This architectural modification effectively eliminates the risk of falling objects and can be readily implemented in public buildings. Furthermore, drone charging and docking stations can be integrated above this barrier to support reliable and safe operations.

III. System Architecture

To support accessibility-focused indoor navigation, the proposed system utilizes an AI-enabled drone that guides users along safe and accessible paths while dynamically adapting to changing environmental conditions. The overall architecture is illustrated in Figure 1. At the core of the system is the educational RoboMaster Tello Talent drone, developed by DJI [18]. This compact, lightweight platform ($\sim$90 g) is equipped with a built-in camera and supports programmable control through a Software Development Kit (SDK). The drone communicates wirelessly with a Ground Control System (GCS) over a Wi-Fi network using the User Datagram Protocol (UDP). Live video streams captured by the drone are transmitted to the GCS, where they are processed by the object detection algorithm. Based on this analysis, the GCS issues navigation commands to the drone, enabling it to guide users reliably toward their intended destinations.

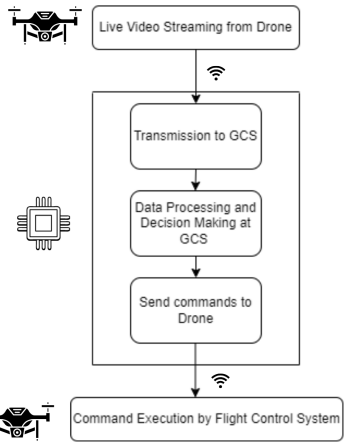

Figure 1. System architecture of the proposed drone-based navigation system, illustrating the drone, wireless communication with the GCS, real-time object detection, and navigation command feedback for guiding users along accessible routes.

While the long-term objective is to achieve fully onboard processing for autonomous navigation on capable drones, the current implementation strategically uses edge computing to support real-time decision-making in controlled environments. This approach allows us to utilize educational drones while still performing computationally intensive tasks, such as object detection and path planning, with accuracy and efficiency. By offloading these processes to a GCS, we demonstrate the feasibility and effectiveness of our method, establishing

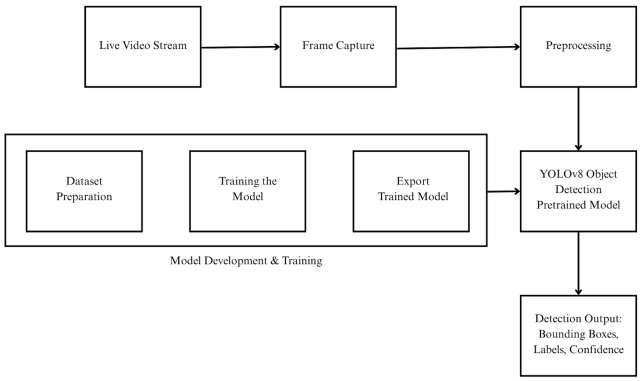

Figure 2. Workflow of the YOLO object detection pipeline used in the proposed drone-based navigation system. The GCS receives live video streams from the drone and processes each frame using the pre-trained YOLO model [20].

a strong foundation for future deployment on more advanced platforms.

IV. Accessibility-Oriented Object Detection using Drones

In this section, we focus on the object detection procedure. A key component in developing a real-time *Drone Accessibility Assistant* for individuals with mobility impairments is the implementation of an efficient object detection algorithm. For this purpose, You Only Look Once (YOLO) [19] was selected due to its high speed and accuracy. YOLO formulates object detection as a single-stage regression problem, eliminating the complexity and latency of traditional multi-stage pipelines.

Figure 2 illustrates the YOLO workflow, beginning with live video capture from the drone and continuing through frame preprocessing, dataset preparation, model training, and export. The trained model is then deployed for YOLOv8-based object detection, which generates bounding boxes, labels, and confidence scores. The ground control station receives the live video streams and processes each frame using the pre-trained YOLO model [20]. To enable rapid prototyping and efficient training, we used Google Colab as the development platform, utilizing its cloud-based resources to accelerate model training and improve inference performance.

A dataset consisting of over 4,500 images was collected from various sources, including [21][22][23]. The distribution of image categories is illustrated in Figure 3. The top-left bar chart shows the number of instances for each class: accessibility symbol, person, potholes, ramps, and stairs. The top-right plot overlays all bounding boxes to visualize their spatial coverage. The bottom heatmaps represent the distribution of bounding box center coordinates (x, y) and their width–height dimensions across the dataset. Each image was manually annotated to identify regions of interest corresponding to target objects relevant to accessibility, such as stairs, ramps, and potholes.

The YOLOv8-medium model from the Ultralytics library [24] was trained for 60 epochs with an input size of 640 pixels in a Google Colab environment. Model performance

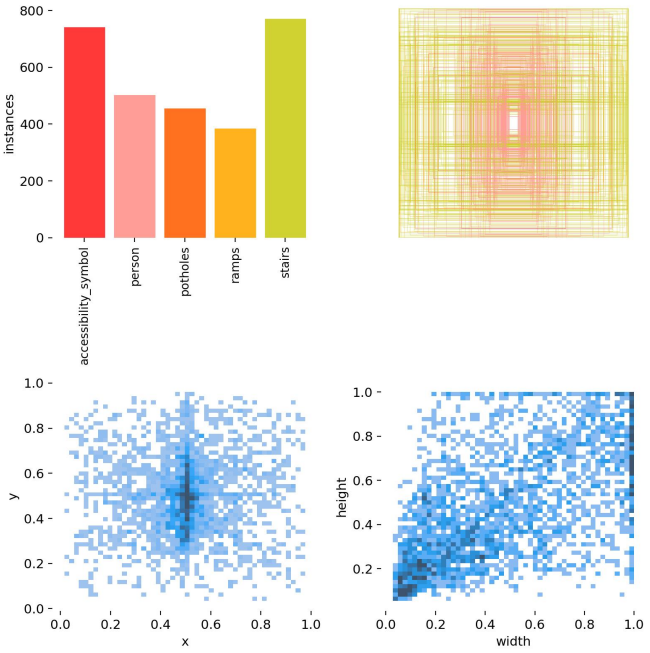

Figure 3. Dataset visualization for accessibility object detection. Top-left: class distribution; top-right: bounding box overlay; bottom-left: bounding box centers; bottom-right: bounding box dimensions.

was evaluated using precision, recall, and mean average precision (mAP) on a validation set. Final predictions on the test set were generated with a confidence threshold of 0.5.

The object detection model demonstrated good performance, achieving a mean average precision (mAP) of 80% at an Intersection over Union (IoU) threshold of 0.5. As illustrated in the confusion matrix (Figure 4), the model indicates robust capability in acurately identifying instances of accessibility symbols (93%) and stairs (90%), with moderate performance on ramps (85%), potholes (73%), and persons (70%). An important area requiring improvement is the model's handling of the background class. As illustrated in the confusion matrix, multiple true instances from other object classes, such as person and potholes, were misclassified as background. These false negatives suggest that the model occasionally fails to detect the presence of an object, instead attributing it to the background class, thus inflating background predictions. Conversely, there are cases where true background pixels were incorrectly classified as object classes, resulting in false positives. These misclassifications reflect a limitation in the model's ability to reliably differentiate between objects of interest and true background. To address this, we prioritize improving the quality of background annotations and increasing the representation of frequently confused background regions during training. These enhancements are crucial for boosting the model's overall precision and recall across all classes.

Figure 5 presents a series of plots illustrating the model's performance evolution over approximately 60 training epochs. These graphs provide critical insights into the learning process, convergence, and generalization capabilities of the model.

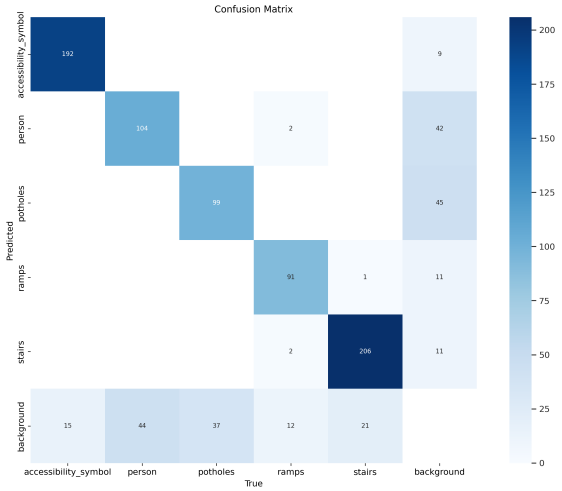

Figure 4. Confusion matrix illustrating the performance of the trained model across all classes. The diagonal values represent correctly classified instances, while the off-diagonal values indicate misclassifications between classes.

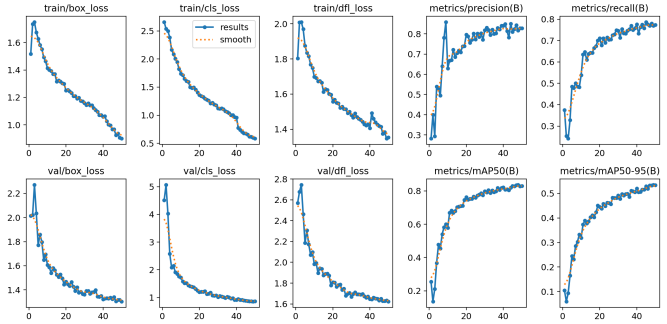

Figure 5. Training and validation performance of the YOLOv8 model across epochs, showing convergence through reduced loss and improved accuracy, demonstrating effective generalization to unseen data.

The top row of plots displays the training loss metrics. All three curves exhibit a consistent and continuous downward trend throughout the training epochs. This steady decrease in training loss indicates that the model is effectively learning from the training data and improving its ability to accurately localize objects (box loss), classify them correctly (classification loss), and refine its distribution focal loss.The smoothness of these curves suggests a stable training process, free from significant oscillations or divergence, which is indicative of appropriate hyperparameter selection and model architecture.

The bottom row of plots details the validation loss metrics and key performance indicators. Similar to the training losses, the validation loss curves demonstrate a steady decline, eventually stabilizing towards the latter epochs. This crucial observation indicates that the model is generalizing well to unseen data, effectively avoiding overfitting to the training set. The continuous improvement in validation performance reinforces the model's robustness and its capacity for real-world application.

Furthermore, the performance metrics showcase significant progress over time. Both *metrics/precision(B)* and *metrics/recall(B)* exhibit a strong upward trajectory, stabilizing at high values by the end of training. This suggests that the model is becoming both more selective, making fewer false positive predictions, and more comprehensive in identifying true positives. The mean average precision metrics offer a more comprehensive assessment of detection performance. In particular, *metrics/mAP50(B)*, evaluated at an IoU threshold of 0.50, shows rapid and sustained improvement, achieving a high score confirming the model's effectiveness in identifying objects with moderate overlap. More critically, *metrics/mAP50-95(B)*, which averages performance across IoU thresholds from 0.50 to 0.95, also exhibits steady gain. Although this metric naturally yields lower values due to stricter localization requirements, its continuous upward trend signifies the model's increasing accuracy in both object detection and localization. The continued rise of this metric suggests that additional training epochs could further refine bounding box precision and overall model performance.

In summary, the combined analysis of the confusion matrix and the training/validation metrics demonstrates the strong performance of the developed model. The confusion matrix reveals high true positive rates across key target object classes, while also identifying the background class as a primary source of misclassifications. This presents an area for targeted refinement, specifically, improving the model's ability to distinguish between actual objects and true background. Concurrently, the training and validation curves demonstrate the model's effective learning and successful generalization, with consistent improvement in all key performance indicators, including precision, recall, and mean average precision.

While publicly available data sources provided a practical basis for developing and evaluating our models, we acknowledge potential domain inconsistencies and inherent dataset biases. Future work will focus on improving dataset relevance and reducing biases, for example by collecting additional domain-specific images or incorporating crowdsourced annotations. We also plan to address class imbalance through data augmentation and sampling strategies. Beyond data considerations, we aim to to enhance detection performance through hyperparameter tuning and advanced training strategies, particularly for underperforming classes. Addressing background-related confusion through methods, such as data augmentation, improved annotation quality, hard negative mining, or context-aware object detection offers a promising direction for improving the model's accuracy and real-world robustness.

V. Dynamic Path Navigation Algorithm

In alignment with our system design objectives, we developed a *Dynamic Path Navigation Algorithm* to enhance drone's autonomous navigation capabilities through real-time environmental perception and adaptive decision-making in dynamic indoor environments. Central to the system is the drone's ability to autonomously scan its surroundings, detect obstacles, and dynamically determine an alternative route, thereby ensuring efficient and safe path navigation.

Algorithm 1 Dynamic Path Navigation Algorithm for Autonomous Drone Guidance

```
procedure GRAPHCONSTRUCTION
    Construct accessibility-compliant graph G = (V, E)
    return G
procedure HANDLEOBSTACLE(G, current_node, next_node, destination)
    RemoveEdge(G, current_node, next_node)
    P ← Dijkstra(current_node, destination)
    return P
procedure NAVIGATE(source, destination)
    G ← GraphConstruction()
    current_node ← source
    P ← Dijkstra(current_node, destination)
    while current_node ≠ destination do
        next_node ← NextNode(P)
        if ObstacleDetected(current_node, next_node) then
            P ← HandleObstacle(G, current_node, next_node, destination)
        else
            current_node ← next_node
    Display "Arrived at Destination"
```

We assume the availability of prior information about the premises, such as an initial floor map of the building, to construct a graph-based representation of the navigable environment. Specifically, the environment is modeled as a directed graph $G = (V, E)$, where vertices V represent key decision points from which the drone can move in various directions (e.g., intersections, turns, or locations of interest), and edges E denote traversable connections between them. Each edge carries a weight reflecting the cost or distance of traversal.

This graph serves as the operational blueprint for path planning. Given a source node and a destination node, the algorithm computes an optimal route using Dijkstra's algorithm. As the drone follows the computed path, it continuously monitors the environment to detec and respond to unexpected obstacles in real time. If an obstruction is detected along the next segment of the planned path, the algorithm dynamically updates the graph by removing the blocked edge and recalculating an alternative shortest path from the current node to the destination. The process iterates until the drone reaches the destination node, at which point it signals successful arrival.

Algorithm 1 provides a detailed step-by-step description of this adaptive path-planning framework, which integrates classical graph-based planning with real-time environmental perception to enable reliable, obstacle-aware navigation in dynamic indoor settings.

In the following, we first analyze the algorithm's worst-case time complexity, providing insight into its computational efficiency. We then present a discussion on its completeness, demonstrating that the algorithm is guaranteed to find a path if one exists in the graph.

Theorem 1. *The worst-case runtime of our Dynamic Path Navigation algorithm is $O(\mathcal{E} \cdot (|V| + |E|)log|V|)$ in the worst case.*

Proof. The overall time complexity of the Dynamic Path Navigation algorithm is driven by two primary operations: the computation of the shortest path using Dijkstra's algorithm and the real-time obstacle detection mechanism during path execution.

Initially, the algorithm computes the shortest path from the source to the destination node on a pre-constructed graph $G = (V, E)$, where V represents decision points and E denotes traversable edges. In the event of encountering unexpected obstacles during navigation, the algorithm dynamically removes the affected edge from the graph and recomputes the shortest path from the current node to the destination. Let $\mathcal{E}$ denote the total number of such path recalculations triggered by obstacle detections.

Using a priority queue implementation (e.g., binary heap), the time complexity of Dijkstra's algorithm for a single invocation is

$$O\left((|V| + |E|) \log |V|\right).$$

Therefore, across all $\mathcal{E} \leq |E|$ recomputations, the total cost of path planning becomes:

$$O\left(\mathcal{E} \cdot (|V| + |E|) \log |V|\right).$$

In addition, the drone performs a constant-time obstacle check while traversing each edge along the path. In the worst-case scenario, every edge in the graph may be evaluated at least once for obstacle presence, contributing an additional linear cost of $O(|E|)$ for real-time sensing and reaction.

Thus, the total worst-case time complexity of the navigation algorithm is:

$$O\left(\mathcal{E} \cdot (|V| + |E|) \log |V| + |E|\right).$$

This complexity reflects the integration of classical graph-based planning with adaptive, sensor-driven updates, enabling robust and responsive indoor navigation in dynamic environments. □

We now present the completeness guarantee of the proposed path navigation algorithm in Theorem 2. We assume that the drone initiates the algorithm at the source node s, with the objective of reaching the destination node d.

Theorem 2. *If there exists at least one unblocked path from the source node s to the destination d at any time during execution, then the Dynamic Path Navigation Algorithm will reach d in finite time.*

Proof. The algorithm begins by computing the shortest path from the current node to the destination node using Dijkstra's algorithm. Dijkstra's algorithm is complete and optimal for graphs with non-negative edge weights, and thus will return a valid path if one exists in the initial graph.

As the drone follows this path, it continuously monitors the immediate next edge for obstacles. If an obstacle is detected on edge (u, v), the edge is removed from the graph, and the algorithm recomputes the shortest path from the current node u to the destination d using Dijkstra's algorithm on the updated graph.

At each iteration, the graph becomes a subgraph of the original, with potentially fewer edges due to obstacle-induced removals. If a valid path exists from the current node to the destination in the updated graph, Dijkstra's algorithm will find it. The algorithm terminates either when the destination is reached or when no path exists in the current subgraph.

Consequently, as long as at least one unblocked path exists from the current node to the destination, the algorithm will eventually find and traverse it. Upon reaching d, the algorithm halts successfully, establishing completeness under this assumption.

□

VI. Conclusions and Future work

This study introduces an innovative AI-assisted drone-based navigation system aimed at supporting individuals with mobility impairments as they navigate complex indoor environments. By integrating a customized object detection model with dynamic path planning, the system enables real-time identification of accessibility features and obstacles, allowing autonomous aerial robots to guide users along safe and accessible routes. Experimental evaluations conducted in a controlled setting demonstrate the system's feasibility and potential to address critical gaps left by traditional, static navigation tools. The findings showcase the critical role that aerial robotics can play in improving independent mobility, reducing navigational barriers, and advancing inclusion within built environments. The ability of the system to adaptively re-route users in response to environmental changes further reflects its applicability to real-world settings where accessibility needs are both pressing and variable. Future work may focus on improving the accuracy and adaptability of the object detection model to perform reliably across a variety of architectural settings. Refinements to the overall system design, encompassing both software and hardware components, combined with evaluations beyond controlled environments to account for real-world factors, such as lighting variability, human presence, ceiling obstructions, and operational safety, will strengthen scalability and reliability. Pilot deployments or simulation-based validations can further increase credibility and readiness for broader adoption.

References

[1] W. Jeamwatthanachai, M. Wald, and G. Wills, "Indoor navigation by blind people: Behaviors and challenges in unfamiliar spaces and buildings", *British Journal of Visual Impairment*, vol. 37, no. 2, pp. 140–153, 2019.

[2] Z. Cattaneo and T. Vecchi, *Blind vision: the neuroscience of visual impairment*. MIT press, 2011.

[3] M. D. Messaoudi, B.-A. J. Menelas, and H. Mcheick, "Review of navigation assistive tools and technologies for the visually impaired", *Sensors*, vol. 22, no. 20, p. 7888, 2022.

[4] B. Kuriakose, R. Shrestha, and F. E. Sandnes, "Tools and technologies for blind and visually impaired navigation support: A review", *IETE Technical Review*, vol. 39, no. 1, pp. 3–18, 2022.

[5] A. Blattner, Y. Vasilev, and B. Harriehausen-Mühlbauer, "Mobile indoor navigation assistance for mobility impaired people", *Procedia Manufacturing*, vol. 3, pp. 51–58, 2015.

[6] F. J. Rafful Garfias and V. Namboodiri, "Mablesim: A simulation framework for studying accessibility challenges for people with disabilities within indoor environments", in *Proceedings of the 21st International Web for All Conference*, 2024, pp. 23–32.

[7] C. Prandi, B. R. Barricelli, S. Mirri, and D. Fogli, "Accessible wayfinding and navigation: A systematic mapping study", *Universal Access in the Information Society*, vol. 22, no. 1, pp. 185–212, 2023.

[8] C. Loitsch, K. Müller, C. Engel, G. Weber, and R. Stiefelhagen, "Accessiblemaps: Addressing gaps in maps for people with visual and mobility impairments", in *International Conference on Computers Helping People with Special Needs*, Springer, 2020, pp. 286–296.

[9] M. M. Nasralla, I. U. Rehman, D. Sobnath, and S. Paiva, "Computer vision and deep learning-enabled uavs: Proposed use cases for visually impaired people in a smart city", in *Computer Analysis of Images and Patterns: CAIP 2019 International Workshops, ViMaBi and DL-UAV, Salerno, Italy, September 6, 2019, Proceedings 18*, Springer, 2019, pp. 91–99.

[10] R. Khemmar, M. Gouveia, B. Decoux, and J.-Y. y Ertaud, "Real time pedestrian and object detection and tracking-based deep learning. application to drone visual tracking", in *WSCG'2019-27. International Conference in Central Europe on Computer Graphics, Visualization and Computer Vision'2019*, Západočeská univerzita, 2019.

[11] Amazon, *Amazon prime air: Revolutionizing delivery with drones*, Available at: here, Accessed: Aug. 24, 2025, 2025.

[12] MarketDigits, *Drone market outlook 2023-2030: Growth, trends, and insights*, Available at: here, Accessed: Aug. 25, 2025, Dec. 2023.

[13] M. Avila, M. Funk, and N. Henze, "Dronenavigator: Using drones for navigating visually impaired persons", in *Proceedings of the 17th International ACM SIGACCESS Conference on Computers & Accessibility*, 2015, pp. 327–328.

[14] C. Iuga, P. Drăgan, and L. Buşoniu, "Fall monitoring and detection for at-risk persons using a uav", *IFAC-PapersOnLine*, vol. 51, no. 10, pp. 199–204, 2018.

[15] E. Mangina, E. O'Keeffe, J. Eyerman, and L. Goodman, "Drones for live streaming of visuals for people with limited mobility", in *2016 22nd International Conference on Virtual System & Multimedia (VSMM)*, IEEE, 2016, pp. 1–6.

[16] T. Castelli, A. Sharghi, D. Harper, A. Tremeau, and M. Shah, "Autonomous navigation for low-altitude uavs in urban areas", *arXiv preprint arXiv:1602.08141*, 2016.

[17] Y. Wang and W. Chen, "Path planning and obstacle avoidance of unmanned aerial vehicle based on improved genetic algorithms", in *Proceedings of the 33rd Chinese Control Conference*, IEEE, 2014, pp. 8612–8616.

[18] DJI, *Robomaster tt*, Accessed: Sep. 2, 2025, 2024.

[19] J. Redmon, S. Divvala, R. Girshick, and A. Farhadi, "You only look once: Unified, real-time object detection", in *Proceedings of the IEEE conference on computer vision and pattern recognition*, 2016, pp. 779–788.

[20] N. Aswini and S. Uma, "Custom based obstacle detection using yolo v3 for low flying drones", in *2021 International Conference on Circuits, Controls and Communications (CCUBE)*, IEEE, 2021, pp. 1–6.

[21] Ö. Alparslan, A. Özcan, and Ö. Çetin, "Model ve veri odaklı yaklaşımlar ile nesne tespit başarısının arttırılmasına yönelik esa ve veri seti optimizasyonları", *Mühendislik Bilimleri ve Araştırmaları Dergisi*, vol. 4, no. 2, pp. 121–128, 2022.

[22] *Google images*, https://images.google.com/, Accessed: Sep. 10, 2025.

[23] Coco, *Comon objects in context*, https://cocodataset.org/, Accessed: Sep. 10, 2025.

[24] G. Jocher and the Ultralytics Team, *Ultralytics yolov8*, Accessed: Sep. 10, 2025, 2023.